Available online at www.sciencedirect.com
ScienceDirect
Journal of Crystal Growth 298 (2007) 687–690
JOURNAL OF CRYSTAL GROWTH
www.elsevier.com/locate/jcrysgro

GaN/AlGaN active regions for terahertz quantum cascade lasers grown by low-pressure metal organic vapor deposition

G.S. Huang[a], T.C. Lu[a], H.H. Yao[a], H.C. Kuo[a,*], S.C. Wang[a], Greg Sun[b], Chih-wei Lin[c], Li Chang[c], Richard A. Soref[d]

[a]*Department of Photonics & Institute of Electro-Optical Engineering, National Chiao Tung University, 1001 TA Hsueh Road, Hsinchu, 300 Taiwan, ROC*
[b]*Department of physics, University of Massachusetts, Boston, MA 02125, USA*
[c]*Department of Materials Science and Engineering, National Chiao Tung University, 1001 TA Hsueh Road, Hsinchu, 300 Taiwan, ROC*
[d]*Air Force Research Laboratory, Sensors Directorate, Hanscom AFB, MA 01731, USA*

Available online 22 November 2006

Abstract

The GaN/AlGaN active regions for terahertz (THz) quantum cascade lasers were grown by metal organic chemical vapor deposition (MOCVD). The surface of the sample was characterized by atomic force microscopy (AFM). The structure of this sample was evaluated by X-ray diffraction (XRD) and transmission electron microscopy (TEM). The XRD pattern and cross-sectional TEM images showed that a well-controlled quantum cascade GaN/AlGaN layers could be prepared. Optical properties of the active region of a terahertz GaN/AlGaN have been investigated by Fourier transform infrared (FTIR) spectrometer. It was found that the frequency of E_1(LO) phonon decreased in quantum cascade GaN/AlGaN structures. The phonon frequency shift could be attributed to the effect of phonon zone folding.

PACS: 81.15.Gh; 73.61.Ey; 61.10.Nz; 68.37.Lp

Keywords: A1. X-ray diffraction; A3. Metal organic chemical vapor deposition; B1. Nitrides

1. Introduction

Recently, considerable effort has been expanded to develop a solid-state coherent source in the terahertz (THz) range. Semiconductor THz intersubband lasers have been proposed for several material systems [1–3] and were recently demonstrated in the GaAs/AlGaAs material system using a quantum cascade scheme [4–11]. In the GaAs-based material system, this implies that the energy separation between the lower laser state and the ground state where the majority of electrons reside is just above the LO-phonon energy (~36 MeV), which is comparable to room temperature k_BT (~26 MeV). Obviously, a material system with a large LO-phonon energy will be desirable for the high-temperature operation of THz quantum cascade lasers (QCLs). Sun et al. [12] proposed to use a GaN-based system with large LO-phonon energy (~90 MeV) for THz QCLs. The advantages are threefold. First, the large LO-phonon energy in a GaN-based system can reduce the thermal population of the lower laser state. Second, ultrafast LO-phonon scattering in GaN/AlGaN QWs can be used for the rapid depopulation of the lower laser state [12,13]. Third, the large LO-phonon energy can also increase the lifetime of the upper laser state by reducing the relaxation of electrons with higher in-plane kinetic energy via emission of a LO-phonon. Sun et al.'s [12] analysis of their structure has shown that a relatively low threshold current density of 832 A/cm^2 can provide a threshold optical gain of 50 cm^{-1} at room temperature. Moreover, the characteristic temperature is estimated to be as high as 136 K.

Although QCL structures have been reported, these samples were grown by molecular beam epitaxy (MBE) and hot wall epitaxy (HWE). Metal organic chemical vapor deposition (MOCVD) should offer several advantages over

*Corresponding author.
E-mail address: hckuo@faculty.nctu.edu.tw (H.C. Kuo).

0022-0248/$ - see front matter © 2006 Elsevier B.V. All rights reserved.
doi:10.1016/j.jcrysgro.2006.10.106

MBE and HWE for QCL fabrication, including higher growth rates, easier reactor maintenance and mass production. In this study, we used a MOCVD system to grow GaN/AlGaN active regions for the THz QCLs designed by Sun et al. [12]. Atomic force microscopy (AFM), X-ray diffraction (XRD), transmission electron microscopy (TEM) and Fourier transform infrared (FTIR) spectrometer were used to characterize the grown samples. The flat sample surface and abrupt layer interfaces were demonstrated and the frequency shift of the E_1(LO) phonon was discussed.

2. Experiments

All the samples in this work were grown in a low-pressure vertical (EMCORE D75) reactor with a high-speed rotation of the susceptor. The reagents were pure ammonia, trimethylgallium (TMGa) and trimethylaluminum (TMAl). Hydrogen and nitrogen purified by purifier were used as the carrier gases. The rotating speed was 900 rpm. *C*-plane sapphire epi-ready substrates were used for all the growth.

The group III and V precursors were separated in two manifolds and mixed before they entered the reactor. Before material growth, the sapphire substrate was annealed to remove any residual impurities on the surface in H_2 ambient at 1100 °C for 5 min. For all samples, a normal 30-nm-thick GaN nucleation layer was deposited at 500 °C. Then the temperature was raised up to 1100 °C for growth of a 2-μm-thick GaN buffer layer. Before the structures were grown, the ambient gas was changed into nitrogen with hydrogen and the ratio of two carrier gases was kept constant. The schematic structure of the active region of quantum cascade laser is shown in Fig. 1. The full structure consisted of 20 periods of quantum wells with each period consisting of three GaN QWs and three $Al_{0.2}Ga_{0.8}N$ barriers with layer thickness (nm): 3/**4**/3/**2.5**/2/**2.5** (wells in bold and barriers in plain). The surface morphology and epitaxial thickness of multi-layer were measured by AFM and TEM. The XRD pattern of the active regions was measured and simulated by using a Bede Scientific D1 double-crystal XRD. The infrared reflectivity spectra were collected at room temperature by a Bomen FTIR spectrometer. We used nonpolarized light with an incident angle of 75° (Brewster's angle was about 68°) and a Fourier transform spectrometer, equipped with a KBr beam splitter and a mercurcy–cadmium–tellride detector cooled down to 77 K.

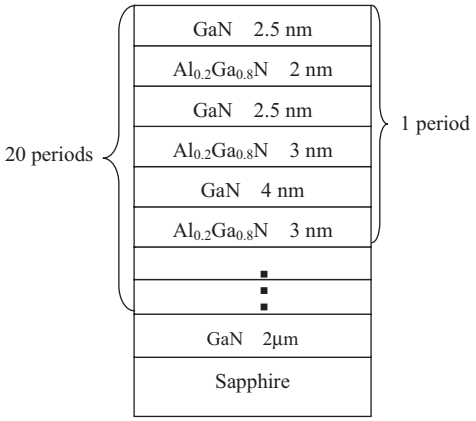

Fig. 1. Schematic diagram of the AlGaN QCL active layer structure.

3. Results and discussion

Fig. 2 shows an AFM image of the same sample. The average roughness measured by AFM was less than 1 nm over a $5 \times 5\,\mu m^2$ surface area, which was comparable to that of a high-quality GaN epilayer.

Fig. 3 shows a cross-sectional TEM image of the 20-period QC structure and each period consisting of three GaN QWs and three $Al_{0.2}Ga_{0.8}N$ barriers. In Fig. 3(a), a contrast made by the periodically aligned 20 sets of the MQWs can be seen. No dislocations running across the sample are observable in this figure. In Fig. 3(b), bright parts and dark parts correspond to the AlGaN barriers and the GaN wells, respectively. It is obviously seen that the interfaces are very sharp. The actual layer thickness of the GaN QWs and $Al_{0.2}Ga_{0.8}N$ barriers can be obtained from the TEM pictures. The thickness difference between the grown sample and the design structure was less than 0.5 nm.

The crystalline quality of the samples was evaluated by (0 0 0 2) symmetric high-resolution X-ray diffraction (HRXRD) with a Cu K_{a1} radiation. The average thicknesses of the AlGaN barriers and the GaN wells were determined by the angular distance using satellite peaks of $\omega/2\theta$-scan diffraction patterns. The HRXRD pattern of the $\omega/2\theta$-scan (0 0 0 2) reflections for QC structure is shown in Fig. 4. The top and bottom lines show the experimental and simulated results, respectively. The satellite peaks due to the QC structure can be clearly seen up to the 4th order;

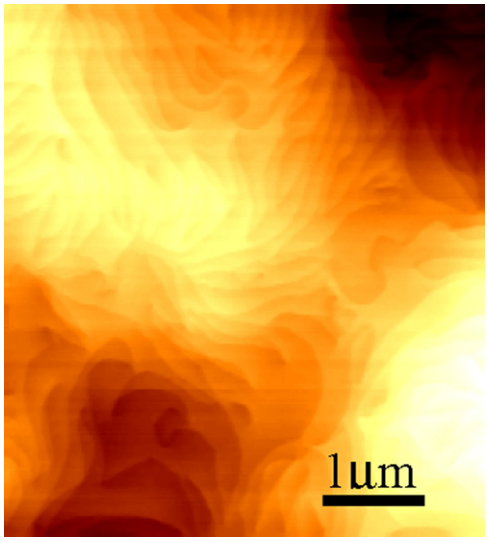

Fig. 2. AFM top-view image of the grown AlGaN/GaN QC structure.

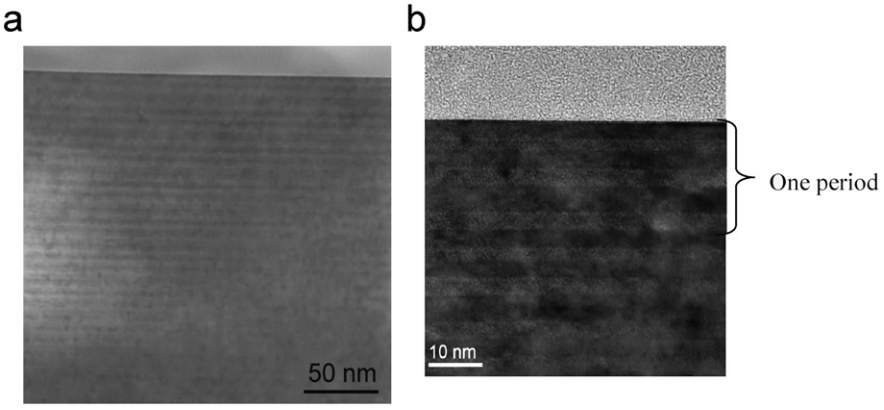

Fig. 3. (a) Cross-sectional TEM images of 20 periods MQW sample. (b) Two periods with each period consisting of three GaN QWs and three AlGaN barriers with layer thickness (nm): 3/**4**/3/**2.5**/2/**2.5** (wells in bold and barrier in plain).

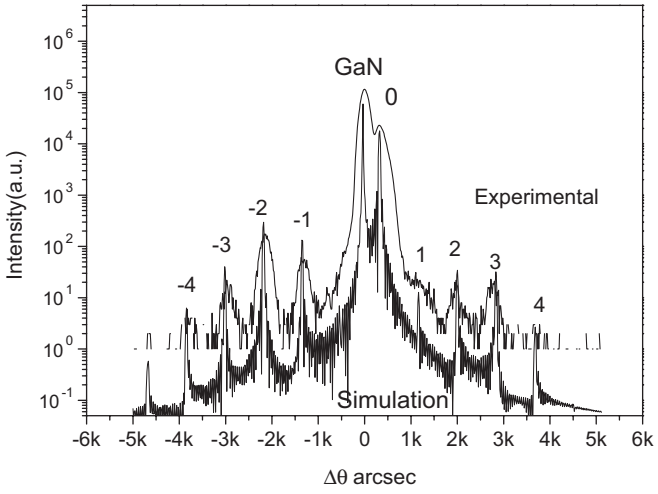

Fig. 4. (0 0 0 2) ω–2θ X-ray diffraction pattern and simulated result of the AlGaN/GaN QCL active region structure.

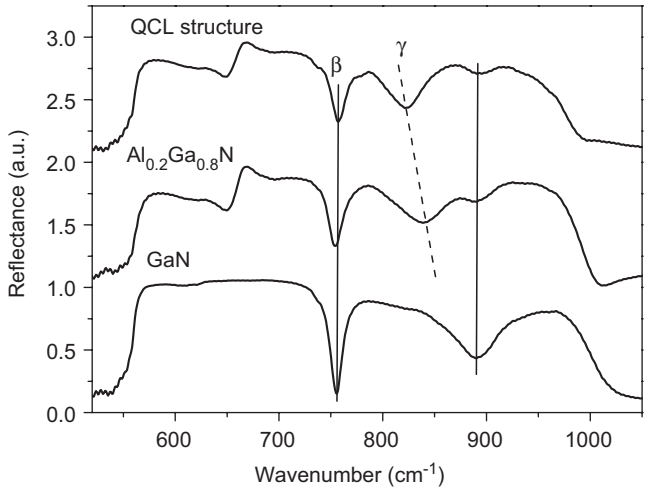

Fig. 5. Room temperature FTIR of the QCL structure, $Al_{0.2}Ga_{0.8}N$ epilayer and GaN bulk.

Table 1
Simulation results of X-ray diffraction pattern

Layer	Thickness (nm)	Material	Composition
1	2.9	GaN	
2	2.4	$Al_xGa_{1-x}N$	0.20
3	2.9	GaN	
4	3.6	$Al_xGa_{1-x}N$	0.20
5	4.5	GaN	
6	3.6	$Al_xGa_{1-x}N$	0.20

peaks indicates that smooth and abrupt interfaces with good periodicity of the QC structure for the 20 cascading periods. Table 1 lists the simulated thicknesses and compositions of epilayers in one period. The good agreement between the experimental curve and the simulated data confirm the successful fabrication of a QC structure.

Fig. 5 shows measured FTIR spectra for a GaN film, an AlGaN with a GaN buffer and a QCL structure with a GaN buffer deposited on sapphire substrates. Two dips labeled as β, γ with frequencies of 758 and 890 cm^{-1}, respectively, originate from GaN and sapphire [14]. The dips labeled with dashed line were assigned as a E_1(LO) phonon. Note that as a consequence of the periodic superlattice in the active region, the FTIR frequency of the E_1(LO) phonon shifted as shown in Fig. 5. The optical phonon dispersion curve of the E_1 phonon mode can be represented by the expression [15]

$$\omega(q) = \omega(0) - \Delta\omega \sin^2\left(\frac{qa}{4}\right), \quad (1)$$

where a is the lattice parameter, which is the average period thickness in the active region, q is the phonon wave number, $\omega(0)$ is zone-center phonon frequency and $\Delta\omega$ is the difference between the zone-center and the zone-boundary frequencies of the phonon dispersion curve of interest. In the present calculations $\omega(0)$ is taken to be 839 cm^{-1} [14]. The phonon frequency shift can be calculated to be 19.9 cm^{-1} [15], which agrees with the measured frequency shift (17 cm^{-1}) between the E_1 phonon

mode in the active region and the E_1 phonon frequency obtained in the $Al_{0.2}Ga_{0.8}N$ film. As a result, the phonon frequency shift can be explained by the effect of zone-folding in the periodic active structures.

4. Conclusion

In summary, we grew high crystalline quality GaN/AlGaN active regions of QCL by low-pressure MOCVD. The morphologies of full active regions were quite smooth. The compositional data of $Al_xGa_{1-x}N$ were determined and the active layer structure of QCL was successfully grown and investigated. The FTIR measurement demonstrated the zone-folding in the phonon frequency due to the sharpness of the interface between the barrier and well layers in the active region of the GaN/AlGaN QCL structure.

Acknowledgments

This work was supported by the MOE ATU program and in part by the National Science Council of Republic of China (ROC) in Taiwan under contract Nos. NSC 94-2120-M-009-007 and NSC 94-2215-E-009-082 and US Air Force Research Laboratory.

References

[1] G. Sun, Y. Lu, J.B. Khurgin, Appl. Phys. Lett. 72 (1998) 1481.
[2] L. Friedman, G. Sun, R.A. Soref, Appl. Phys. Lett. 78 (2001) 401.
[3] R.A. Soref, G. Sun, Appl. Phys. Lett. 79 (2001) 3639.
[4] C. Sirtori, Nature 417 (2002) 132.
[5] R. Köhler, A. Tredicucci, F. Beltram, H.E. Beere, E.H. Linfield, A.G. Davies, D.A. Ritchie, R.C. Lotti, F. Rossi, Nature 417 (2002) 156.
[6] M. Rochat, L. Ajili, H. Willenberg, J. Faist, Appl. Phys. Lett. 81 (2002) 1381.
[7] G. Scalari, S. Blaser, L. Ajili, J. Faist, H. Beere, E. Linfield, D. Ritchie, G. Davies, Appl. Phys. Lett. 83 (2003) 3453.
[8] S. Barbieri, J. Alton, S.S. Dhillon, H.E. Beere, M. Evans, E.H. Linfield, A.G. Davies, D.A. Ritchie, R. Köhler, A. Tredicucci, F. Beltram, IEEE J. Quantum Electron. 39 (2003) 586.
[9] B.S. Williams, H. Callebaut, S. Kumar, Q. Hu, J.L. Reno, Appl. Phys. Lett. 82 (2003) 1015.
[10] B.S. Williams, S. Kumar, H. Callebaut, Q. Hu, J.L. Reno, Appl. Phys. Lett. 83 (2003) 5142.
[11] S. Kumar, B.S. Williams, S. Kohen, Q. Hu, J.L. Reno, Appl. Phys. Lett. 84 (2004) 2494.
[12] G. Sun, R.A. Soref, J.B. Khurgin, Superlattice. Microstruct. 37 (2005) 107.
[13] J.D. Heber, C. Gmachl, H.M. Ng, A.Y. Cho, Appl. Phys. Lett. 81 (2002) 1237.
[14] G.S. Huang, T.C. Lu, H.H. Yao, H.C. Kuo, S.C. Wang, unpublished.
[15] M. Rajalakshmi, A.K. Arora, Nanostruct. Mater. 11 (1999) 399.